

# Temperature-insensitive compact phase-shifted long-period gratings induced by surface deformation in single-mode fiber

Shijie Zheng<sup>1,2</sup> · Xiaohua Lei<sup>3</sup> · Yinian Zhu<sup>4</sup>

Received: 6 August 2015 / Accepted: 15 September 2015 / Published online: 23 September 2015  
© Springer-Verlag Berlin Heidelberg 2015

**Abstract** We present a temperature-insensitive compact phase-shifted long-period grating (PS-LPG) induced by using focused pulse CO<sub>2</sub> laser via point-by-point technique. By introducing a phase shift with 1800° ( $\pi$  shift) in the center of the long-period grating ( $\sim$ 420  $\mu\text{m}$  per period, 20 periodicity in total), the original coupling resonance at 1318.55 nm splits into two symmetrical spectral peaks at 1283 and 1348 nm. FWHM between those two peaks is 36.55 nm, and the power intensities of two peaks are the same as  $-10.2$  dB. The thermal characteristic of the PS-LPGs is around 8.8 pm/°C that is less than that of fiber Bragg grating (12 pm/°C). As a result, such fiber grating devices can be applied in a laser cavity as an all-fiber filter. Variation of phase shifts in LPGs give rise to different spectral peaks of coupled resonance, which makes the proposed PS-LPGs as a good candidate for the applications in sensing networks and optical telecommunications.

## 1 Introduction

Long-period grating (LPG), which couples the guided fundamental core mode to the forward-propagating cladding modes in a single-mode fiber, is a type of power transmission grating [1]. Unlike fiber Bragg grating (FBG), the periodicity that is perturbed with refractive index in LPGs is from 100 to 1000  $\mu\text{m}$  so that they can be easily fabricated [2]. LPGs have been so far employed in telecommunications and sensing applications as spectral-selective filters due to advantages in ultra-low attenuation, small back-reflection, and insensitivity of polarization [3]. There are a lot of practical applications of LPGs in dense wavelength-division-multiplexed optical communications and sensing networks [4–8], including gain-flattening in erbium-doped fiber amplifier and all-fiber switching in telecommunications. Various optical fiber components and devices have been configured and fabricated; however, the study on PS-LPGs and its real applications in abovementioned fields are few [9, 10]. The gain-flattening fiber filter has been theoretically derived by Qian and Chen [11] with the PS-LPG, but it can only flatten two peaks. It is also reported that the ultrasonic and acoustic emission can be detected by utilizing a phase-shifted FBG [12, 13]. Furthermore, such PS-LPGs have been suggested for high-power couplers that can be applied in microstructured optical fiber lasers [14]. Also, as small transmission with narrow bandwidth can be generated, such PS-LPG can form optical cavity because it acts as a wavelength selecting-component for one of the mirror at the end and reflects the light back to form the resonator. Some researchers used UV light through amplitude mask to fabricate the PS-LPGs [15, 16], while others employed CO<sub>2</sub> laser or electric arc to manufacture the PS-LPGs in photonic crystal fibers (PCFs) [17, 18]. In

✉ Shijie Zheng  
zhengshijie@hit.edu.cn

<sup>1</sup> Key Lab of Structures Dynamic Behavior and Control of the Ministry of Education (Harbin Institute of Technology), Harbin 150090, China

<sup>2</sup> School of Civil Engineering, Harbin Institute of Technology, Harbin 150090, China

<sup>3</sup> Key Lab for Optoelectronic Technology and System of the Ministry of Education Chongqing University, Chongqing 400044, China

<sup>4</sup> Department of Mechanical Engineering, Northwestern University, Evanston, IL 60208, USA

this work, we present the fabrication of PS-LPGs by using focused pulses of CO<sub>2</sub> laser via point-by-point technique. The method can be practically used by softening the fiber with heat and deforming the cross section.

### 2 Operation principle of PS-LPG

As long as we divide the non-uniform FBGs into several periodicities, we can solve the transfer matrix via coupled-mode theory. It is specifically used for calculating LPG, as the periods in LPGs are much less (compared to FBGs). An illustration of LPG periodicity is shown as Fig. 1, where  $n_1$  stands for the unperturbed core refractive index and  $n_1 + dn$  stands for the perturbed, respectively;  $n_2$  stands for the refractive index in cladding;  $L_1$  and  $L_2$  are the lengths for each region.

The core mode can be coupled with the cladding mode in perturbed region:

$$\Lambda = 2\pi / (\beta_1 - \beta_2) \tag{1}$$

where  $\Lambda$  is the grating periodicity, and  $\beta_1$  and  $\beta_2$  are the propagating constants for the unperturbed and perturbed regions, respectively. Coupled-mode equations in perturbed region can be given as:

$$\frac{dA_1}{dZ} = -j(\beta_1 A_1 + CA_2) \tag{2}$$

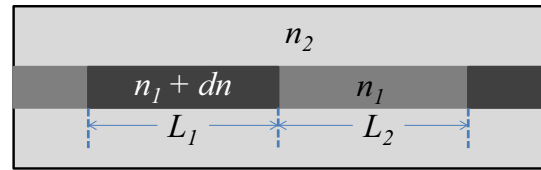


Fig. 1 Scheme for illustration of periodicity in the LPG

$$\frac{dA_2}{dZ} = -j(CA_1 - \beta_2 A_2) \tag{3}$$

where  $A$  is the amplitude for the coupling mode and  $C$  is the coupling coefficient expressed as:

$$C = k \frac{\oint_{A_{co}} \varphi_1(r, \phi) \varphi_2(r, \phi) dA_{co}}{\oint_{A_{co}} |\varphi_1|^2 dA_{co}} \tag{4}$$

In it,  $\varphi$  is the transverse field vector for  $A$ ;  $A_{co}$  stands for the area for the core cross section;  $k = 2\pi/\Lambda L$  is the coupling coefficient constant. The transfer matrix for perturbed region can be obtained by developing Eqs. (2) and (3), as follows:

$$M_p = \begin{bmatrix} m_{11} & m_{12} \\ m_{21} & m_{22} \end{bmatrix} \tag{5}$$

$$m_{11} = \frac{1}{2} \left\{ 1 - 1 / \left[ 1 + \left( \frac{2C}{\beta_1 - \beta_2} \right)^2 \right]^{1/2} \right\} \exp \left\{ -jL_2 \left\{ (\beta_1 - \beta_2) / 2 - C \left[ 1 + \left( \frac{\beta_1 - \beta_2}{2C} \right)^2 \right]^{1/2} \right\} \right\} + \frac{1}{2} \left\{ 1 + 1 / \left[ 1 + \left( \frac{2C}{\beta_1 - \beta_2} \right)^2 \right]^{1/2} \right\} \exp \left\{ -jL_2 \left\{ (\beta_1 - \beta_2) / 2 + C \left[ 1 + \left( \frac{\beta_1 - \beta_2}{2C} \right)^2 \right]^{1/2} \right\} \right\} \tag{6}$$

$$m_{22} = \frac{1}{2} \left\{ 1 + 1 / \left[ 1 + \left( \frac{2C}{\beta_1 - \beta_2} \right)^2 \right]^{1/2} \right\} \exp \left\{ -jL_2 \left\{ (\beta_1 - \beta_2) / 2 - C \left[ 1 + \left( \frac{\beta_1 - \beta_2}{2C} \right)^2 \right]^{1/2} \right\} \right\} + \frac{1}{2} \left\{ 1 - 1 / \left[ 1 + \left( \frac{2C}{\beta_1 - \beta_2} \right)^2 \right]^{1/2} \right\} \exp \left\{ -jL_2 \left\{ (\beta_1 - \beta_2) / 2 + C \left[ 1 + \left( \frac{\beta_1 - \beta_2}{2C} \right)^2 \right]^{1/2} \right\} \right\} \tag{7}$$

$$m_{12} = m_{21} = \frac{1}{2} \left\{ 1 / \left[ 1 + \left( \frac{2C}{\beta_1 - \beta_2} \right)^2 \right]^{1/2} \right\} \begin{bmatrix} \exp \left\{ -jL_2 \left\{ (\beta_1 - \beta_2) / 2 - C \left[ 1 + \left( \frac{\beta_1 - \beta_2}{2C} \right)^2 \right]^{1/2} \right\} \right\} \\ - \exp \left\{ -jL_2 \left\{ (\beta_1 - \beta_2) / 2 + C \left[ 1 + \left( \frac{\beta_1 - \beta_2}{2C} \right)^2 \right]^{1/2} \right\} \right\} \end{bmatrix} \tag{8}$$

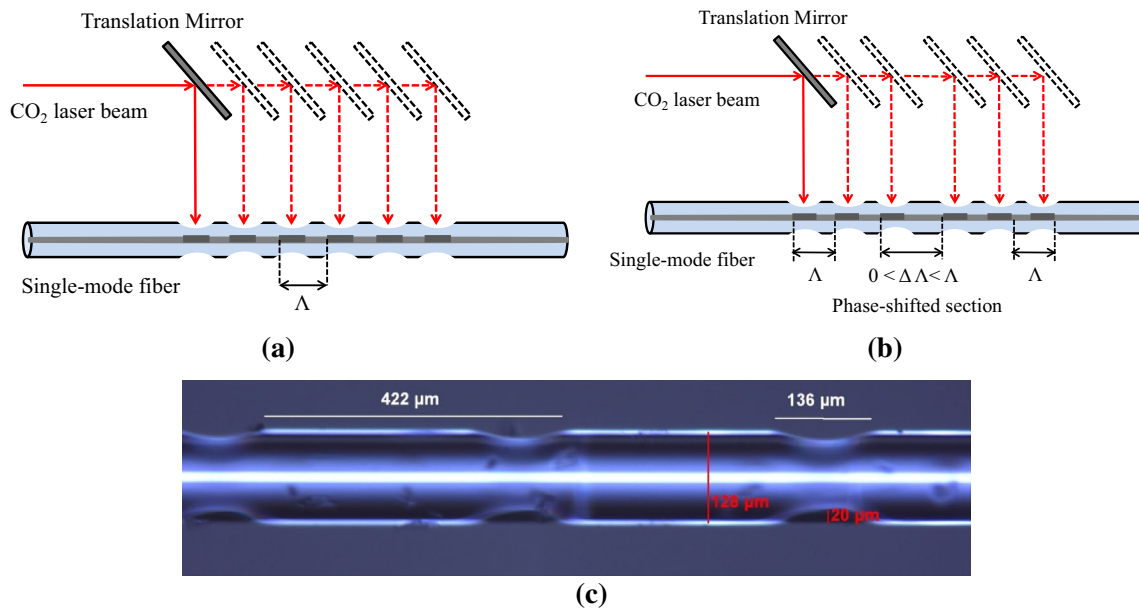


**Fig. 2** Fabrication of **a** LPGs and **b** PS-LPG; **c** Microscope image of LPGs with periodicity ~420 μm via point-by-point technique

The transfer matrix in the unperturbed region can be expressed by

$$M_u = \begin{bmatrix} \exp(-j\beta_1 L_1) & 0 \\ 0 & \exp(-j\beta_2 L_1) \end{bmatrix} \quad (9)$$

The transfer matrix in the whole length of the LPG can be obtained by the concatenation of the transfer matrices of all the grating periodicity, which can be presented by

$$M = \begin{bmatrix} i_{11} & i_{12} \\ i_{21} & i_{22} \end{bmatrix} = M_{p(n)} \times M_{u(n)} \times M_{p(n-1)} \times \dots \times M_{p(1)} \times M_{u(1)} \quad (10)$$

where  $|i_{11}|^2$  is the power intensity transmission of the guided fundamental core mode.

$$M_{PS-LPG} = M_{p(n)} \times M_{u(n)} \times \dots \times M_{p(n/2)} \times M_{u(n/2)} \times M_s \times M_{p(n/2-1)} \times M_{u(n/2-1)} \times \dots \times M_{p(1)} \times M_{u(1)} \quad (12)$$

A standard PS-LPG has a pair of LPGs with identical length of periodicity in fiber. A distance in range of  $0 < \Delta\Lambda < \Lambda$  ( $\Delta\Lambda =$  phase shift) is added to separate those two kinds of LPGs. Harumoto et al. [8] suggested that the mode re-coupling can be used in PS-LPG if the LPGs were in a distance of  $\Lambda$  or less. As  $L_1$  and  $L_2$  are the lengths of the first and second LPG ( $L_1$  and  $L_2$  are in multiples of  $\Lambda$ ), transfer matrix for PS-LPG with  $\theta = 2\pi\Delta\Lambda/\Lambda$  and length  $L = L_1 + \Delta\Lambda + L_2$  as well as guided fundamental core mode  $A$  and the  $LP_{0m}$  cladding mode  $B^{(m)}$  can be expressed as:

$$\begin{bmatrix} A(L_0 + L_2) \\ B^{(m)}(L_0 + L_2) \end{bmatrix} = \begin{bmatrix} e^{j(\delta^{(m)} - \chi_{core}/2)L_2} M_1 & e^{j(\delta^{(m)} - \chi_{core}/2)L_2} e^{-j(\theta - 2\delta^{(m)}L_0)} M_2 \\ -e^{-j(\delta^{(m)} + \chi_{core}/2)L_2} e^{-j(\theta - 2\delta^{(m)}L_0)} M_2^* & e^{-j(\delta^{(m)} + \chi_{core}/2)L_2} M_1^* \end{bmatrix} \times \begin{bmatrix} A(L_0) \\ B^{(m)}(L_0) \end{bmatrix} \quad (13)$$

A phase shift can be generated by adding a length of unperturbed region in the center of an LPG. In the PS-LPG, a matrix should be presented as

$$M_s = \begin{bmatrix} \exp(-j\beta_1 L_s) & 0 \\ 0 & \exp(-j\beta_2 L_s) \end{bmatrix} \quad (11)$$

which must be inserted into (10), where  $L_s$  is the length of the region added into the LPG. The transfer matrices in the whole PS-LPG can be obtained by

where  $L_0 = L_1 + \Delta\Lambda$  and  $j = \sqrt{-1}$ .  $M_1$  and  $M_2$  are expressed as follows:

$$M_1 = -j \frac{\phi^{(m)}}{\sqrt{\phi^{(m)2} + \kappa^{(m)2}}} \sin \frac{\sqrt{\phi^{(m)2} + \kappa^{(m)2}}}{2} L + \cos \frac{\sqrt{\phi^{(m)2} + \kappa^{(m)2}}}{2} L \quad (14)$$

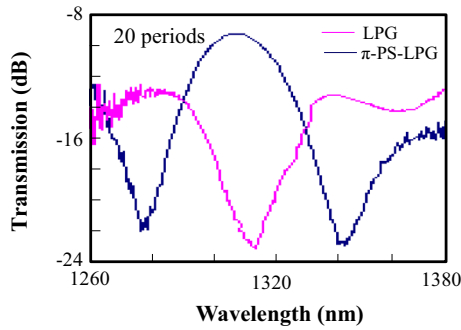


**Fig. 3** Transmission spectra profiles of LPG and PS-LPG with  $\pi$ -phase shift at the grating center

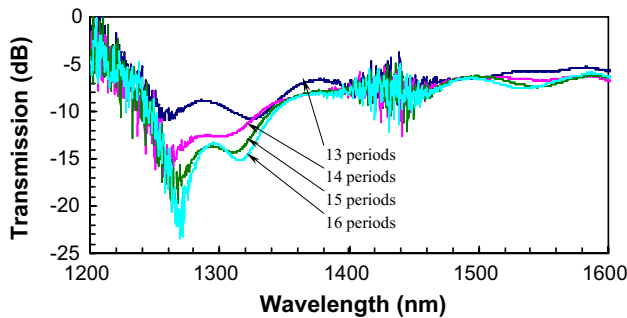


**Fig. 4** Transmission spectra evolution of PS-LPG by half  $\pi$ -phase shift (13–16 periods)

$$M_2 = -j \frac{\kappa^{(m)}}{\sqrt{\phi^{(m)^2 + \kappa^{(m)^2}}} \sin \sqrt{\frac{\phi^{(m)^2 + \kappa^{(m)^2}}{2}} L \quad (15)$$

where  $\beta_{\text{core}}$  and  $\beta_{\text{cladding}}^{(m)}$  are propagation coefficients of the core mode and the  $\text{LP}_{0m}$  cladding mode;  $\kappa^{(m)}$  is the cross-coupling coefficient;  $\delta^{(m)} = \frac{1}{2}(\beta_{\text{core}} - \beta_{\text{cladding}}^{(m)} - \frac{2\pi}{\Lambda})$  and  $\phi^{(m)} = 2\delta^{(m)} + \chi_{\text{core}}$ .

### 3 Inscription of PS-LPG

Figure 2 presents the fabrication process of LPGs, PS-LPG, and the real image of such gratings inscribed on optical fiber. A  $\text{CO}_2$  laser with galvanometer was employed for directing and focusing laser beam to  $\sim 130\text{-}\mu\text{m}$  Gaussian focal spot. We use an optical spectrum analyzer with measurement wavelength region from 1200 to 1600 nm to trace the transmission spectrum profiles in situ. The heating point created by  $\text{CO}_2$  laser can be designed on the fiber by point-by-point writing method. When fiber is moved to a new position by translation stage, the laser is turned on so that light beam can scan across. This surface deformation

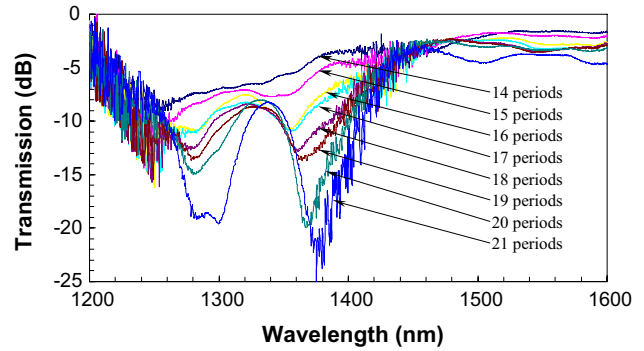


**Fig. 5** Transmission spectra evolution of  $\pi$ -PS-LPG at 4/21 length of grating (14–21 periods)

causes reduction in diameter of the fiber. We use standard single-mode fiber to manufacture the PS-LPGs with periodicity  $\sim 420\ \mu\text{m}$ .

### 4 Experimental results and discussions

Figure 3 shows the LPG with a dip of  $-8.81\ \text{dB}$  and full-width at half-maximum of  $15.91\ \text{dB}$  as well as the resonance wavelength at  $1318\ \text{nm}$ . This LPG was induced with only 10 periodicities (a total length of  $4.6\ \text{mm}$ ). We introduced a  $\pi$ -phase shift into the tenth periodicity of the grating with a total number of 20 periodicities (a total length of  $9.4\ \text{mm}$ ). Two symmetrical rejection bands are at wavelengths of  $1283$  and  $1348\ \text{nm}$  with left dip of  $-11.212\ \text{dB}$  and right dip of  $-11.857\ \text{dB}$ . A band-pass width between the dips is  $36.55\ \text{nm}$ , shown in Fig. 3. Inserting a blankness of half periodicity in center of the grating causes the conversion of destructive interference into constructive interference at phase-matching wavelength.

Figure 4 expresses the transmission spectra profiles of half  $\pi$  PS-LPG at grating center, 16 periodicities in total. It was observed that at the thirteenth periodicity, both resonances were in the same peak attenuation. As more gratings inscribed, the attenuation of lower resonance peak increases faster than that of the higher resonance peak. The values of  $-22.94$  and  $-15.01\ \text{dB}$  have been obtained for the lower and higher resonance peaks at the sixteenth periodicity. The transmission spectra profile of PS-LPG shown in Fig. 5 is a  $\pi$  shift in the center of the fourth and fifth, with 21 periodicities written. It was difficult to identify a clear peak at the fourteenth periodicity at the beginning. With more gratings written, the resonance becomes definite. Two troughs of similar attenuation, with small span, were noticed. This result agrees with the theoretical work [16]. To explore the thermal stability, Fig. 6a shows the PS-LPG transmission spectra profiles with multiple  $\pi/2$ -phase shifts at grating center at temperatures of  $23$  and  $190\ ^\circ\text{C}$ , respectively.

**Fig. 6** **a** Transmission spectra profiles of a  $\pi$ -PS-LPG at 23 and 190 °C and **b** resonance wavelength of *left* dip of the  $\pi$ -PS-LPG against temperature

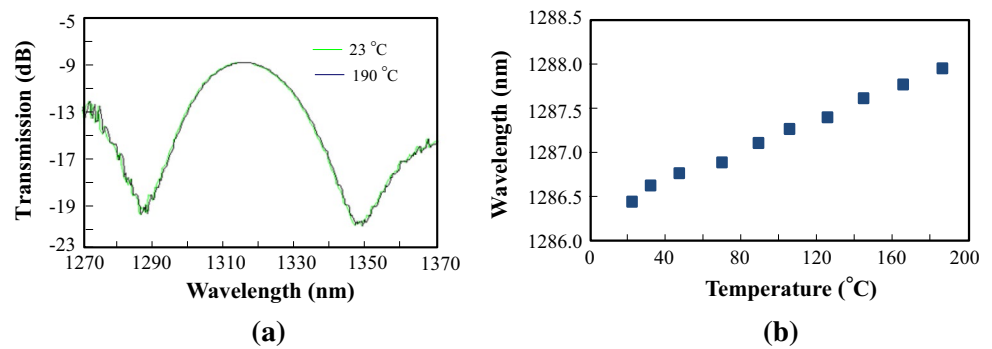


Figure 6b shows the dependence of the resonance wavelength at left dip of the  $\pi$ -PS-LPG on temperature. The left dip shift from 23 to 190 °C is around 1470 nm. The thermal characteristic of this PS-LPG is about 8.8 pm/°C. Compared to the thermal sensitivity of FBG (12 pm/°C), the proposed PS-LPG is more thermal stable.

## 5 Conclusion

We fabricated several PS-LPGs by surface deformation by using CO<sub>2</sub> laser via point-by-point technique. The rejection band peaks are stable in resonance strength and operating wavelength, demonstrated in the temperature range of 23–190 °C. The CO<sub>2</sub>-laser-induced PS-LPGs are compact and are good candidates for lifetime and high-temperature applications in sensing applications or fiber optical communications.

**Acknowledgments** This research work has been supported by Natural Science Foundation of Heilongjiang under (Grant Number QC2015048); by China Postdoctoral Science Foundation under (Grant Number 2014M560265), (Grant Number 2015T80356).

## References

1. A.M. Vengsarkar, P.J. Lemaire, J.B. Judkins, V. Bhatia, T. Erdogan, J.E. Sipe, Long-period fiber gratings as band-rejection filters. *J. Lightwave Technol.* **14**, 58–64 (1996)
2. A.M. Vengsarkar, J.R. Pedrazzani, J.B. Judkins, P.J. Lemaire, N.S. Bergano, C.R. Davidson, Long-period fiber-grating-based gain equalizers. *Opt. Lett.* **21**, 336–338 (1996)
3. B. Ortega, L. Dong, W.F. Liu, J.P. de Sandro, High-performance optical fiber polarizers based on long-period gratings in birefringent optical fibers. *IEEE Photon. Technol. Lett.* **9**, 1370–1372 (1997)
4. S. Zheng, Long-period fiber grating moisture sensor with nanostructured coatings for structural health monitoring. *Struct. Health Monit.* **14**(2), 148–157 (2015)
5. S. Zheng, B. Shan, M. Ghandehari, J. Ou, Sensitivity characterization of cladding modes in long-period gratings photonic crystal fiber for structural health monitoring. *Measurement* **72**, 43–51 (2015)
6. S. Zheng, Y. Zhu, S. Krishnaswamy, Fiber humidity sensors with high sensitivity and selectivity based on interior nanofilm-coated photonic crystal fiber long-period gratings. *Sens. Actuators, B* **176**, 264–274 (2013)
7. P.F. Wysocki, J.B. Judkins, R.P. Espindola, M. Andrejco, A.M. Vengsarkar, Broad-band erbium-doped fiber amplifier flattened beyond 40 nm using long-period grating filter. *IEEE Photon. Technol. Lett.* **9**, 1343–1345 (1997)
8. M. Harumoto, M. Shigehara, H. Sugauma, Gain-flattening filter using long-period fiber gratings. *J. Lightwave Technol.* **20**, 329–339 (2002)
9. Y. Zhu, P. Shum, C. Lu, D.M. Lacquet, P.L. Swart, S.J. Spammer, Highly compact and tunable optical add-drop multiplexer in dense WDM network systems. *J. Opt. Netw.* **2**, 370–378 (2003)
10. Y. Zhu, B.M. Lacquet, P.L. Swart, S.J. Spammer, P. Shum, C. Lu, Device for concatenation of phase-shifted long-period grating and its application as gain-flattening fiber filter. *Opt. Eng.* **42**, 1445–1450 (2003)
11. J.R. Qian, H.F. Chen, Gain flattening fiber filters using phase-shifted long-period fiber gratings. *Electron. Lett.* **34**, 1132–1133 (1998)
12. T. Liu, M. Han, Analysis of  $\pi$ -phase-shifted fiber Bragg gratings for ultrasonic detection. *IEEE Sens. J.* **12**, 2368–2373 (2012)
13. A. Rosenthal, D. Razansky, V. Ntziachristos, High-sensitivity compact ultrasonic detector based on a pi-phase-shifted fiber Bragg grating. *Opt. Lett.* **36**, 1833–1835 (2011)
14. F. Prudeniano, L. Mescia, T. Palmisano, M. Surico, M. De Sario, G. Cesare Righini, Optimization of pump absorption in MOF lasers via multi-long-period gratings: design strategies. *Appl. Opt.* **51**, 1410–1420 (2012)
15. O. Deparis, R. Kiyon, O. Pottiez, M. Blondel, I.G. Korolev, S.A. Vasiliev, E.M. Dianov, Bandpass filters based on  $\pi$ -shifted long-period fiber gratings for actively mode-locked erbium fiber laser. *Opt. Lett.* **26**, 1239–1241 (2001)
16. R. Zengerle, O. Leminger, Phase-shifted Bragg-grating filters with improved transmission characteristics. *J. Lightwave Technol.* **13**, 2354–2358 (1995)
17. H. Ke, K.S. Chaing, J.H. Peng, Analysis of phase-shifted long-period fiber gratings. *IEEE Photon. Technol. Lett.* **10**, 1596–1598 (1998)
18. R. Gao, Y. Jiang, L. Jiang, Multi-phase-shifted helical long period fiber grating based temperature-insensitive optical twist sensor. *Opt. Express* **22**, 15697–15702 (2014)